lubricants

MDPI

Article

Effect of Ultrasonic Rolling on Surface Properties of GCr15 Spherical Joint Bearing

Hao Zhang [1], Xiuli Yang [2], Xiqiang Ma [1,3,*], Dongliang Jin [3,4] and Jinyuan You [1]

[1] School of Mechatronics Engineering, Henan University of Science and Technology, Luoyang 471003, China; 18461008951@163.com (H.Z.); yjy878455760@gmail.com (J.Y.)
[2] CCCC Second Harbour Engineering Co., Ltd., Wuhan 430040, China; ya3ngxiuli@ccccltd.cn
[3] Longmen Laboratory, Luoyang 471003, China; ziranheping@163.com
[4] National Joint Engineering Research Center for Abrasion Control and Molding of Metal Materials, Luoyang 471003, China
* Correspondence: maxiqiang@haust.edu.cn

Abstract: Ultrasonic surface rolling process (USRP) has the potential to improve the surface mechanical properties of metal components with platelike or cylindrical macrostructure, but its effect on spherical surfaces remains to be studied in depth. In order to investigate the effect of USRP on the surface roughness, hardness and wear resistance of a spherical joint bearing made of GCr15 bearing steel, ultrasonic rolling strengthening was carried out on a spherical bearing surface under various conditions. The surface roughness and hardness variations of samples before and after strengthening were investigated. It was found that the USRP strengthening process can effectively enhance the surface properties of GCr15 spherical bearing materials, reduce the surface roughness by more than 45%, and increase the surface hardness by more than 10%. Friction and wear tests were carried out before and after ultrasonic rolling. The results show that the friction coefficient of the bearing surface can be reduced by 28%, and that the wear volume can be reduced by 29%. The variation in the friction coefficient correlated to the variance of wear volume as the reinforcement changes.

Keywords: ultrasonic rolling; surface roughness; surface hardness; friction coefficient; wear volume

check for updates

Citation: Zhang, H.; Yang, X.; Ma, X.; Jin, D.; You, J. Effect of Ultrasonic Rolling on Surface Properties of GCr15 Spherical Joint Bearing. *Lubricants* **2024**, *12*, 208. https://doi.org/10.3390/lubricants12060208

Received: 17 May 2024
Revised: 3 June 2024
Accepted: 6 June 2024
Published: 8 June 2024

Copyright: © 2024 by the authors. Licensee MDPI, Basel, Switzerland. This article is an open access article distributed under the terms and conditions of the Creative Commons Attribution (CC BY) license (https://creativecommons.org/licenses/by/4.0/).

1. Introduction

Knuckle bearings are widely used in many industries, such as in the chemical, marine, and electric power industries, and the surface performance of its inner ring is crucial to its service life. The surface ultrasonic rolling strengthening process can be utilized to improve the surface performance of materials and increase their strength, contributing also towards environmental protection, areas which have been of wide concern. Many researchers have used this technology to strengthen the surface properties of steel, aluminum alloy, titanium alloy and other materials [1–3].

During the application of USRP technology, the ultrasonic signal is converted to an electrical signal by the transducer and amplified by the amplitude lever. Finally, the high-frequency mechanical vibration is output on the impact head [4,5], achieving the combination of ultrasonic technology and traditional rolling technology. The high-frequency impact generated by USRP technology causes plastic deformation on the surface layer of the workpiece, producing a "peak" and "valley" effect on the surface. Thus, the surface roughness of the material is reduced, and the surface performance is improved [6]. In addition, due to the dislocation and cell rupture of the material during the USRP process, finer nanocrystals are formed, which can improve the overall performance of the material [7,8]. In terms of research methods, the single-factor test is a common method used to explore the influence of ultrasonic rolling process parameters on strengthening [9]. Some researchers have employed the orthogonal test to assess the degree of mutual interference between different components; using finite element analysis to replace some of the tests in this process can significantly cut test costs [10–12]. Some

researchers also strengthened the pad of the knuckle bearing while carrying out ultrasonic rolling on the inner ring, which further improved mechanical performance [13,14]. In addition to surface roughness, hardness and other intuitive properties, wear resistance is also a critical factor influencing the properties of joint bearings [15], and the evaluation of friction and wear properties is a common method used to investigate these properties [16]. Liu Yu [17] studied the influence of USRP on the friction and wear properties of TB8 titanium alloy and analyzed the structure and properties of the oxide layer formed at the friction area. Han Y [18] studied the wear properties of QAl10-3-1.5 aluminum bronze alloy treated by USRP and evaluated the improvement of the wear resistance in terms of the friction coefficient and wear volume and wear mechanism. Yong D [19] tested the wear performance of high-carbon and high-chromium steel treated by USRP and analyzed the strengthening mechanism of USRP on the sample through the fracture and dissolution mechanism of the primary carbides on the surface after wear. Meigui Y [20,21] performed impact kinetic energy wear tests on the surface of Inconel 690 alloy treated with USRP and explored the impact wear behavior of the samples at different temperatures. Additionally, Meigui Y also conducted friction corrosion tests on the samples to verify the effect of USRP on improving the corrosion resistance of the materials. Peng Z [22] investigated the effect of USRP on the surface integrity and wear resistance of Inconel 718 nickel-based superalloy under a high-pressure coolant supply.

To sum up, the ultrasonic rolling has a significant strengthening effect on the surface properties of metal materials. Previous work mainly focused on components with platelike or cylindrical structures, research on spherical bearing materials is relatively rare. For these workpieces, the curvature of the sample in the direction perpendicular to the ultrasonic tool head may affect the strengthening effect; therefore, research on this kind of material has certain explorative value. To explore the potential of USRP in the inner ring of GCr15 spherical joint bearing, this work carried out a USRP strengthening treatment, tested the hardness and surface roughness of the sample before and after strengthening, and analyzed the influence of process parameters on the strengthening effect. Finally, based on the friction and wear test, the strengthening effect of USRP on the surface wear resistance of the joint bearing was discussed.

2. Materials and Methodology

2.1. Materials

The GCr15 bearing inner ring selected in the test was quenched and finely machined. The hardness of the surface to be strengthened was 53 ± 0.5 HRC, and the roughness was 0.48~0.72 μm. The main chemical composition of the material is shown in Table 1. The outer surface of the bearing inner ring was spherical, and the dimensions are shown in Figure 1 (size unit: mm). In order to explore the strengthening effects of ultrasonic rolling on the surface of the inner ring of the joint bearing, ultrasonic rolling strengthening tests were carried out under various working conditions.

Table 1. The main chemical composition of GCr15 bearing inner ring material used in the test.

Ingredient	C	Mn	Si	S	P	Cr
Proportion (wt%)	0.95~1.05	0.20~0.40	0.15~0.35	≤0.02	≤0.027	1.30~1.65

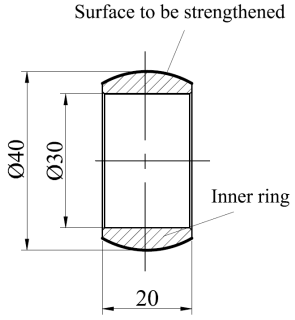
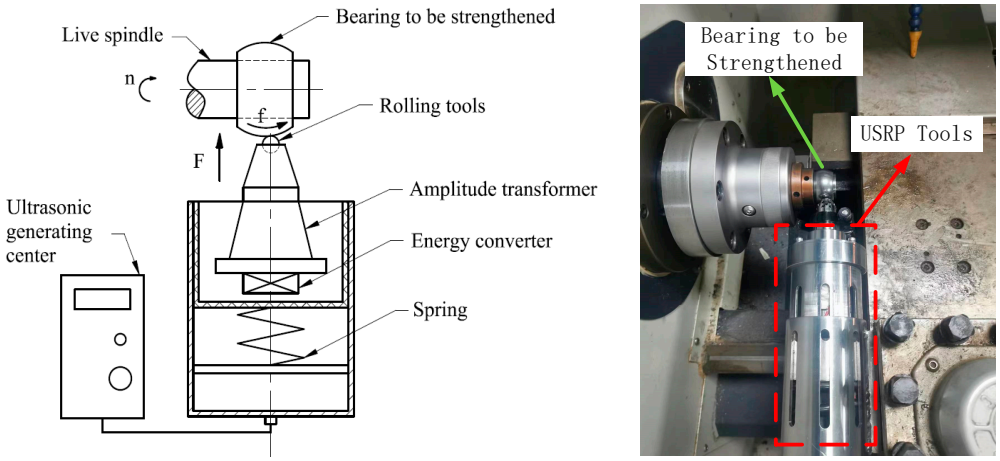


Figure 1. Inner ring dimensions of the bearing in this work.

2.2. USRP Test

Figure 2a shows the schematic of the ultrasonic rolling strengthening apparatus. This work used a horizontal lathe with a special fixture to realize the clamping of bearing samples and the control of speed. The ultrasonic test center (Shanghai Xuanbang Metal New Material Technology Co., Ltd., Shanghai, China) was selected to adjust the amplitude during the ultrasonic rolling process, which mainly consisted of an ultrasonic generation center, transducer, amplitude transformer and rolling tool, and an ultrasonic frequency of 20 kHz. During ultrasonic rolling reinforcement, the rolling tool is installed on the tool holder and the feeding velocity (f) is generated with the feeding movement of the tool holder. Static pressure (F) during the USRP is adjusted by the spring compression in the static rolling tool, and lubricant is used in the strengthening process to improve reinforcement effect. The single-factor test was conducted for two strengthening parameters, e.g., amplitude and static pressure. Table 2 shows the value of the two parameters. During tests, the bearing speed was set at 250 r/min and the ultrasonic tool feeding speed was set at 30 mm/min. To examine the influence of amplitude, the static pressure was fixed at 450 N. In the single-factor test for static pressure, the amplitude was fixed at 15 μm. Figure 2b shows the process of the ultrasonic rolling test.



(**a**) USRP schematic diagram (**b**) USRP physical diagram

Figure 2. Ultrasonic rolling strengthening process.

Table 2. Setting of ultrasonic roll extrusion processing parameters.

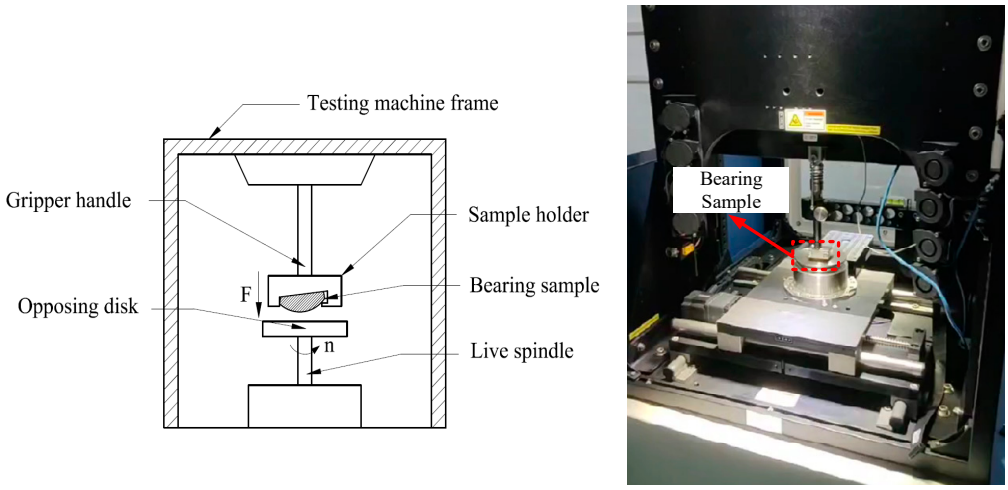
USRP Parameters	**Parameter Value**					
Amplitude (μm)	5	10	15	20	25	/
Static pressure (N)	200	300	400	450	500	600

2.3. Characterization and Wear Tests

Hardness and surface roughness are important properties that affect the fatigue life and lubrication characteristics of the joint bearing studied. An HVS-1000A microhardness tester was selected to test the hardness of the sample; the test pressure was 500 gf and the pressure holding time was 14 s. An LEXT OLS5100 3D laser scanning microscope was used to obtain surface roughness. The surface microstructure was obtained by a scanning electron microscope (SEM, JSM-IT800, JEOL Ltd., Beijing, China).

To investigate the effect of ultrasonic rolling on the wear resistance of joint bearings, the MFT-5000 friction and wear testing machine produced by Rtec intruments Inc. was used with a self-developed fixture for the wear resistance test of the sample. The equipment can record the friction coefficient in real time during the test. The principle of the friction and wear test is shown in Figure 3a. During test, the friction time was set to 40 min, the pressure was 100 N, the speed of the opposing disk was 100 r/min, and the grinding material was

high-strength tungsten steel with a hardness of 88 HRC. The parameter selection was based on the practical application of large-scale spherical joint bearing. Since the surface roughness of the strengthened sample is low, it is difficult to observe large a wear spot on the sample in a short time under good lubrication conditions; therefore, no lubricating medium was used in the friction and wear test. The friction coefficient fluctuated greatly in the initial stage of the test; thus, changes in the friction coefficient over 38~39 min were selected for analysis. The friction and wear test process is shown in Figure 3b.



(**a**) Test principle (**b**) Test process

Figure 3. Ball and disc wear testing machine.

After the friction and wear test, the 3D laser scanning microscope was used to conduct a three-dimensional topography scan on the wear area of the sample and obtain the perimeter data of the wear spot and the wear volume (V) according to the perimeter data. The calculation method is as follows:

$$r = \frac{C}{2\pi}$$

$$h = \sqrt{R^2 - r^2}$$

$$V = \frac{2}{3}\pi R^3 - \int_0^h \pi(R^2 - y^2)dy$$
$$= \pi\left[R^2\left(\frac{2}{3}R - h\right) + \frac{1}{3}h^3\right]$$

where C is the circumference of the wear spot, r is the radius of the wear spot, h is the height from the center of the wear spot to the ball center of the bearing inner ring, R is the outer diameter of the bearing inner ring. Figure 4 provides a supplementary illustration for the calculation.

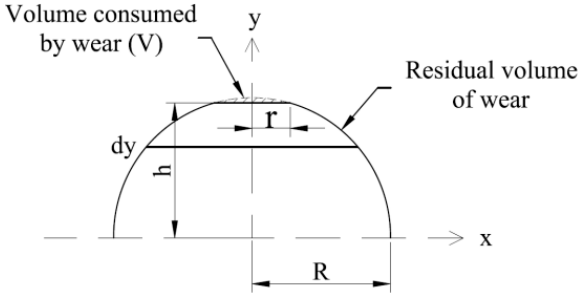


Figure 4. Wear volume calculation diagram.

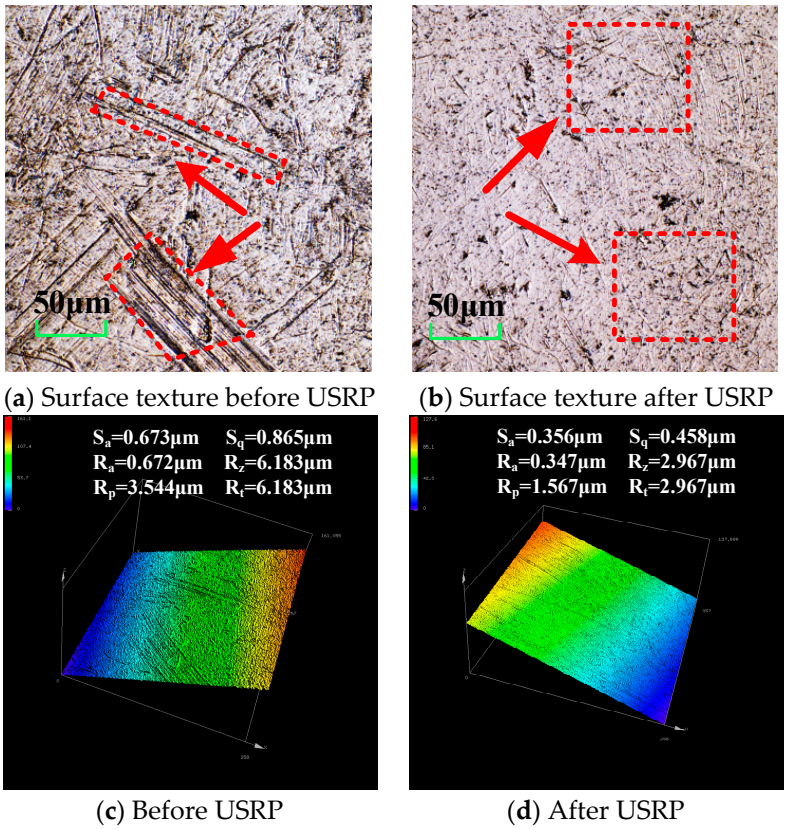
3. Results and Discussion

Since the surface roughness of the samples before strengthening is obviously different, it is misguided to use the surface roughness after strengthening as an evaluation index of the strengthening effect. Therefore, this paper analyzes the reduction value of the surface roughness, and the initial hardness values of the samples of each group are close to each other and fluctuate in a small range around 53 HRC. Therefore, the surface hardness of the sample after strengthening is taken as the objective.

3.1. Strengthening Effect of Ultrasonic Rolling on Surface

3.1.1. Surface Morphology

A 3D laser scanning microscope was used to inspect the sample surface before and after ultrasonic rolling enhancement, as shown in Figure 5.



(**a**) Surface texture before USRP (**b**) Surface texture after USRP

(**c**) Before USRP (**d**) After USRP

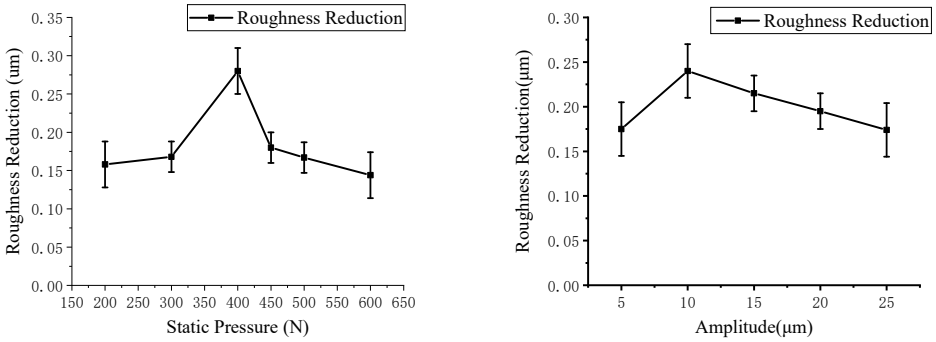
Figure 5. Ultrasonic surface topography of the joint bearing before and after rolling.

After ultrasonic rolling, the surface morphology of the bearing samples is obviously improved, as shown in Figure 5b. The surface of the non-reinforced bearing sample has complex machining textures, which shows long grooves of different depths, and there are a large number of obvious machining textures. The machining grooves in the area marked by the arrows in Figure 5a affect the surface roughness. The strengthened sample is shown in Figure 5b. It can be seen that the processed texture after strengthening still exists, but becomes smaller, and the originally large texture also weakens to some extent at the area marked by the arrow in Figure 5b. Figure 5c is the three-dimensional topography scanning map of the sample before strengthening, with a large number of microscopic protrusions and concave areas, and a relatively rough surface. However, the strengthened sample has significantly reduced microscopic protrusions on the surface, and the overall appearance is smooth, as shown in Figure 5d. The rationale behind this phenomenon lies in the repetitive rolling at a high frequency, which induces plastic deformation in the sample. This process results in the convex surface areas being pressed into the groove, effectively

filling the valleys with the peaks. The peak and valley height difference of the groove on the surface of the material is an important index with which to determine the surface roughness of the sample [23]. The surface roughness of the sample was effectively reduced after strengthening. The reinforced bearing is 0.26~0.49 μm, and the roughness of each group was reduced by 0.1~0.35 μm. The reduction degree was able to reach more than 45%.

3.1.2. Effect of USRP Parameters on Surface Roughness Reduction

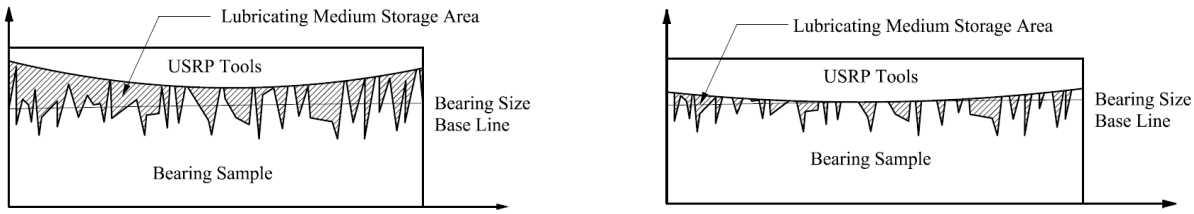
According to the single-factor test, Figure 6a,b shows the influence curves of static pressure and amplitude on the reduction in surface roughness, respectively.



(**a**) Static pressure (**b**) Amplitude

Figure 6. The relationship between static pressure, amplitude, and surface roughness reduction.

Ultrahigh frequency repeated impact is the energy source for reducing the surface roughness of the sample. When the static pressure is too small, the energy of the high frequency vibration of the rolling head cannot be fully transferred to the bearing surface, the plastic deformation of the material is small, and the strengthening effect is not satisfactory. With the increase in static pressure, the impact energy received by the surface increases, the plastic deformation of the material surface increases, and the peak-to-valley effect is enhanced. However, as the static pressure continues to increase, the elastic displacement of the sample increases, and the stability of the strengthening process decreases. At the same time, under a large static pressure, the friction force of the sample surface increases, and the effective storage space of the lubricating medium decreases (as shown in Figure 7). The material structure cut during the strengthening process cannot be completely filled in the trough but sticks to the surface of the material and the surface of the rolling tool. As a result, micro-bumps are generated while the material attached to the surface of the rolling tool produces short micro-grooves on the surface of the sample; thus, the reduction effect of surface roughness becomes worse. As shown in Figure 6, when the static pressure is 400 N, the surface roughness reduction is the highest, ranging from 0.24 to 0.32 μm. Under this static pressure, the impact energy carried by the rolling tool reaches the balancing point, under which the vibration degree of the system is low and sufficient to produce a better peaking and valley filling effect.



(**a**) Low static pressure (**b**) High static pressure

Figure 7. Lubricating medium storage-space diagram.

Similar to the mechanism of the static pressive effect, when the ultrasonic amplitude is small, the impact energy carried by the rolling head is small, and the plastic deformation of the material surface is small. With the increase in amplitude, the reduction effect of surface roughness is higher. However, too large an amplitude makes the movement distance of the rolling head too long, resulting in greater inertia impact, reducing the stability of the strengthening system. At the same time, when the amplitude is large, the effect of the rolling tool cutting material is more obvious, and these material organizations cannot be completely filled in the trough; thus, the strengthening effect is weakened. However, different than the higher static pressure test, the excessive amplitude has a small effect on the deterioration of lubrication conditions during the strengthening process. Therefore, in Figure 6b, the reduction in surface roughness first increases and then decreases with the increase in amplitude. When the amplitude is higher than 10 μm, the downward trend of the roughness strengthening effect is slower than that in Figure 6a. According to the above research, to obtain a better surface strengthening effect, the static pressure of 400 N and the amplitude of 10 μm should be selected as the USRP strengthening parameters.

3.2. Effect of Ultrasonic Rolling on Surface Hardness

The hardness measurement results show that the hardness of the outer surface of the bearing after strengthening is 56~61 HRC, which is 3~7 HRC higher than that before strengthening. Under optimized parameters, the surface hardness of the studied joint bearing can be increased by more than 10%.

Figure 8 shows the strengthening results of surface hardness by static pressure and amplitude. The accumulation of plastic deformation in the process of ultrasonic rolling forms a residual compressive stress field on the surface, resulting in the fracture of the crystal cell and the grain refinement. According to the Hall–Petch theory [24], the refined grain increases the deformation resistance of the grain boundary, which is effective in improving the microhardness of the material. The dislocation movement of material grain boundaries during ultrasonic rolling is also an important factor for surface hardening behavior [25].

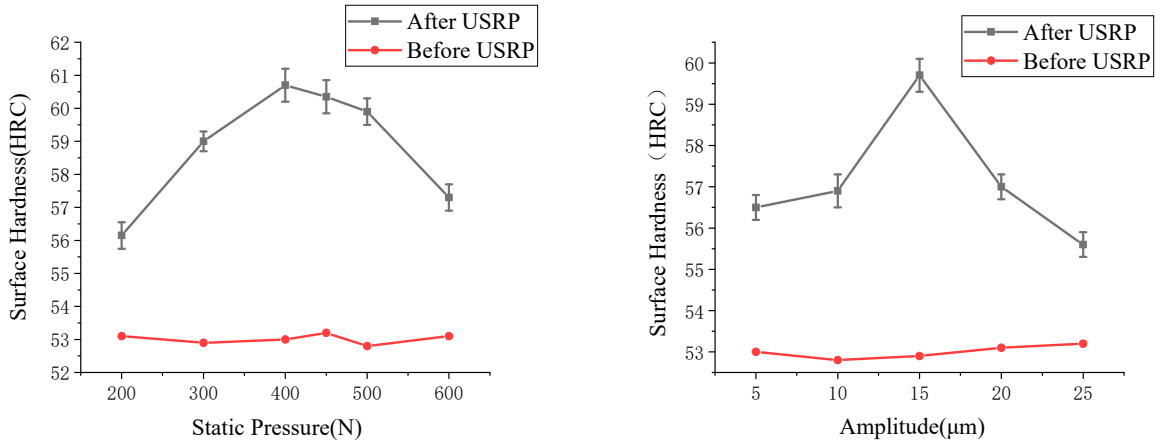


Figure 8. Process parameters and strengthening effect on hardness.

As can be seen from Figure 8a, the surface hardness, which is the difference before and after rolling reinforcement, first increases and then decreases with the elevation in static pressure. When the static pressure is 400 N, the hardness increase effect is better, and the hardening magnitude can reach more than 10%. Under low static pressure, the plastic deformation generated on the specimen surface is small and the residual compressive stress field is relatively low. The stress field may be smaller, the degree of

grain refinement is low, and the hardness enhancement effect is poor. The stability of the system decreases under high static pressure, which makes it difficult to control the uniformity of the introduced residual compressive stress field. Thus, the strengthening effect decreases. As can be seen from Figure 8b, the hardness increase in the bearing materials is limited, the strengthening effect is notably better at amplitudes (15 μm), and the hardening can reach more than 10%. Similar to the strengthening effect of static pressure, the impact energy obtained on the specimen surface gradually increases with the rise in amplitude. The plastic deformation and dislocation movement inside the material increase accordingly. Then, the hardness increases. At a larger amplitude, the impact energy carried by ultrasonic tools is higher, which increases the elastic vibration of bearings and correspondingly increases the dissipation of plastic strain energy, making the distribution of residual compressive stress and dislocation movement difficult to control. Therefore, the hardness enhancement effect decreases at larger amplitudes.

3.3. Effect of Ultrasonic Rolling on Bearing Wear Resistance

A friction and wear test is important to evaluate the wear life of bearings; hardness and roughness are closely related to the wear resistance of bearings. In this work, six groups of bearing samples were selected for the friction and wear test.

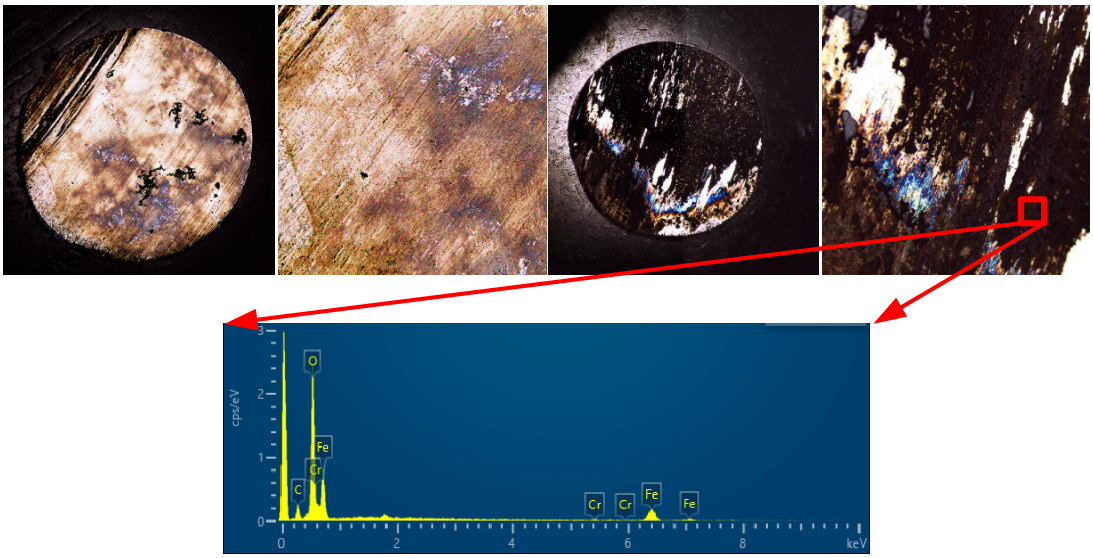
3.3.1. Friction and Wear Test

Under the same test conditions, the morphologies of scratches in the abrasive spot area of the strengthened sample were similar to that before the strengthening, but the erosion magnitude was greatly reduced at the abrasion spot. As can be seen in Figure 9a,b, after a certain time period, the abrasive spot that had not received the strengthening is almost fully covered by oxide, but a large area of metal can still be observed in the abrasive spot that had been strengthened after the same time period. The energy dispersive X-ray spectrometry analysis on the oxide at the abrasive spot was performed, and the spectroscopies are shown in Figure 9a,b. The wight ratio of Fe and O elements are shown in Table 3. The ratio of Fe (71.7%) to O (28.3%) was about 2.5:1 without strengthening, and after strengthening, the ratio of Fe (85.1%) to O (14.9%) increased to 5.7:1; that is, the proportion of the O element in the abrasive spot area is greatly reduced. This indicates that surface strengthening can enhance the erosion resistance of the bearing specimen.

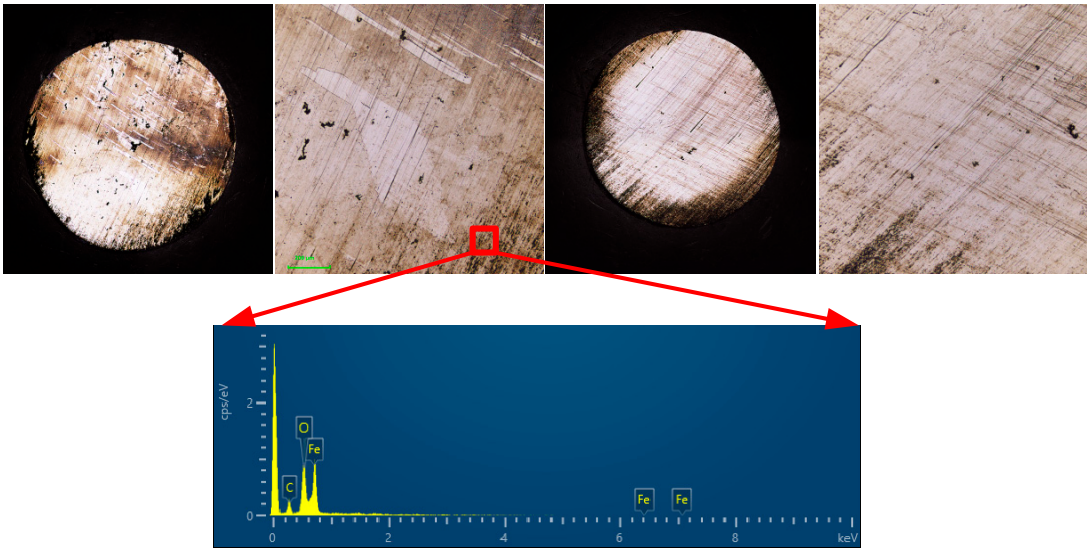
Table 3. Main elements of abrasion spot area.

	Before (wt.%)	**After (wt.%)**
Fe	71.7	85.1
O	28.3	14.9

Figure 10 displays the microstructure of the abrasive spot of the strengthened sample. It can be seen that there are flakes of abrasive debris attached to the surface. Combined with the results in Figure 9, it can be seen that: in the early stage of the friction, there is no lubricating medium. The temperature of the wear area rises rapidly. Then, microscopic wear oxide particles were generated on the surface and adhered to the surface of the sample. As the time increases, the wear particles resulting from friction adhere to one another and accumulate, finally forming abrasive flakes. It can be inferred that the wear mechanisms of the sample are mainly controlled by abrasive wear. The friction and wear test results show that the friction coefficient of the strengthened sample is reduced by 6~28% and the range of the friction coefficient is reduced by more than 30% compared with that without ultrasonic rolling, as shown in Figure 11a. The wear volume is also reduced from 0.31~0.54 mm^3 to 0.23~043 mm^3, as shown in Figure 11b.



(a) Before USRP



(**b**) After USRP

Figure 9. Morphology and elements of abrasive spot in samples before and after strengthening.

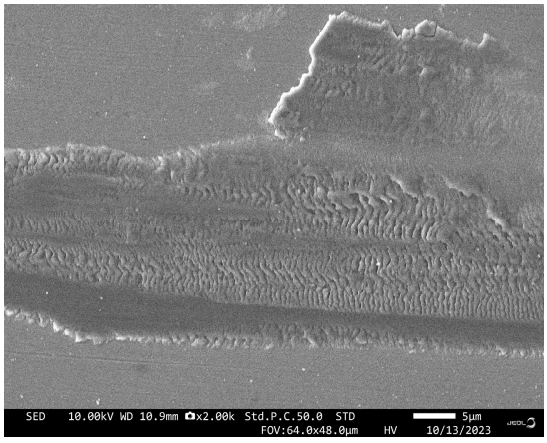
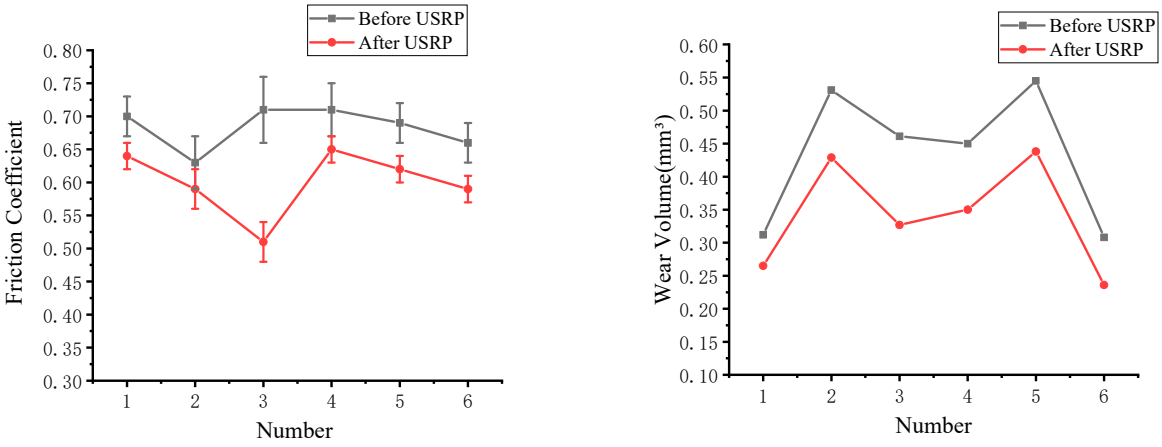


Figure 10. Microstructure of the abrasion area after USRP.



(**a**) Friction coefficient (**b**) Wear volume

Figure 11. Comparison of wear properties of bearing samples before and after reinforcement.

3.3.2. Analysis of Wear Performance

The specimen strengthened by USRP has lower surface roughness and the frictional resistance between the specimen and the grinding disk is smaller. At the same time, the hardness of the specimen strengthened by USRP is higher, and the toughness of the material is increased; thus, the resistance to plastic deformation can be improved [26]. Few abrasive debris and microscopic grooves are generated and the friction coefficient of the specimen strengthened with USRP is reduced. As for the wear volume, it is closely related to the friction coefficient, and a smaller friction coefficient corresponds to a smaller friction resistance. Coupled with higher surface toughness, the wear volume of the strengthened specimen decreases.

It should be noted that USRP has a certain difference in the degree of the reduction in the friction coefficient and wear volume of materials. Taking samples of number 2 and number 3 as an example: after USRP strengthening, the hardness of number 2 has increased greatly (12%); therefore, even though the reduction in the friction coefficient is limited (6.3%), the wear volume reduction effect is still large (19.2%). After USRP strengthening, the effect of the increase in hardness of number 3 is limited (5%); therefore, even though the reduction in the friction coefficient (28%) increased by 21.7% compared with that of number 2, the reduction in the wear volume (29%) was only increased by 9.8% compared with that of number 2. This indicates that the wear resistance of the material is not only related to the variation of the friction coefficient, but also to the hardening of the sample and the improvement in surface roughness, which collectively affect the wear volume of the material.

4. Conclusions

According to the above research and analysis, the following conclusions can be drawn:

(1) USRP has a remarkable strengthening effect on metal materials with a spherical structure. USRP can reduce the surface roughness of the GCr15 knuckle bearing by more than 45% and increase its hardness by more than 10%;

(2) Moderate static pressure and amplitude are feasible to improve the strengthening effect of USRP on the surface roughness and hardness of a GCr15 spherical bearing;

(3) USRP has an obvious effect on decreasing the friction coefficient and increasing the stability of the bearing material, and on reducing the wear volume of the surface material. The average friction coefficient in the stability stage can be reduced by 28%, and the wear volume can be reduced by 29%. When the hardening of the material differs, the optimization of friction coefficient and wear volume of the bearing material by USRP varies.

Author Contributions: Conceptualization, H.Z.; methodology, H.Z. and X.M.; software, D.J.; validation, H.Z. and X.M.; investigation, J.Y.; resources, X.Y.; data curation, H.Z.; writing—original draft preparation, X.M.; writing—review and editing, H.Z.; supervision, D.J.; project administration, H.Z.; funding acquisition, H.Z. All authors have read and agreed to the published version of the manuscript.

Funding: This research was funded by: National Key Research and Development Plan (Grant No. 2021YFB2011000); Longmen Laboratory tuyere industry project (Grant No. LMFKCY2023001); Frontier Exploration Project of Longmen Laboratory (Grant No. LMQYTSKT037). The Key Scientific and Technological Project of Henan Province (Grant No. 242102220081).

Data Availability Statement: The data presented in this study are available on request from the corresponding author due to the authors need to use these data for further studies. So they plan to publish all the trial data after all the studies are completed, and for the time being, they can only communicate them individually to readers who have data requirements.

Conflicts of Interest: Author Xiuli Yang was employed by the company CCCC Second Harbour Engineering Co., Ltd. The remaining authors declare that the research was conducted in the absence of any commercial or financial relationships that could be construed as a potential conflict of interest.

References

1. Cheng, Y.; Wang, Y.; Lin, J.; Xu, S.; Zhang, P. Research status of the influence of machining processes and surface modification technology on the surface integrity of bearing steel materials. *Int. J. Adv. Manuf. Technol.* **2023**, *125*, 2897–2923. [CrossRef]
2. Han, J.; Wang, C.; Song, Y.; Liu, Z.; Sun, J.; Zhao, J. Simultaneously improving mechanical properties and corrosion resistance of as-cast AZ91 Mg alloy by ultrasonic surface rolling. *Int. J. Miner. Metall. Mater.* **2022**, *29*, 1551–1558. [CrossRef]
3. Shahsavar, S.; Ketabchi, M.; Bagherzadeh, S. Fabrication of robust aluminum–carbon nanotube composites using ultrasonic assembly and rolling process. *Int. J. Miner. Metall. Mater.* **2021**, *28*, 160–167. [CrossRef]
4. Liu, C.; Liu, D.; Zhang, X.; He, G.; Xu, X.; Ao, N.; Ma, A.; Liu, D. On the influence of ultrasonic surface rolling process on surface integrity and fatigue performance of Ti-6Al-4V alloy. *Surf. Coat. Technol.* **2019**, *370*, 24–34. [CrossRef]
5. Yin, M.; Yin, H.; Zhang, Q.; Long, J. Effect of ultrasonic surface rolling process on the high temperature fretting wear behavior of Inconel 690 alloy. *Wear* **2022**, *500*, 204347. [CrossRef]
6. Nath, C.; Rahman, M.; Andrew, S.S.K. A study on ultrasonic vibration cutting of low alloy steel. *J. Mater. Process. Technol.* **2007**, *192*, 159–165. [CrossRef]
7. Wang, H.; Wang, X.; Tian, Y.; Ling, Y. Study on microstructure of 42CrMo steel by ultrasonic surface rolling process. *Sci. Rep.* **2023**, *13*, 21289. [CrossRef]
8. Liu, Y.; Li, W.; Sun, Y.; Chen, L.; Chang, G.; Deng, G. Effect of ultrasonic surface rolling process on microstructure and properties of rolled Mg-Y-Nd-Zr alloy. *J. Mater. Sci.* **2023**, *58*, 9362–9381. [CrossRef]
9. Zhou, Z.; Yao, C.F.; Tan, L.; Zhang, Y.; Fan, Y. Experimental study on surface integrity refactoring changes of Ti-17 under milling-ultrasonic rolling composite process. *Adv. Manuf.* **2023**, *11*, 492–508. [CrossRef]
10. Su, C.J.; Xu, T.T.; Zhang, K.; Zhang, K.; Lou, S.M.; Wang, Q. Plastic deformation of magnesium alloy with different forming parameters during ultrasonic vibration-assisted single-point incremental forming. *Rare Met.* **2022**, *41*, 3878–3886. [CrossRef]
11. Minghuan, W.; Shang, Y.; Changshun, L.; Jiajie, W.; Zheng, J.; Xufeng, X. 3D multiphysic simulations of energy field and material process in radial ultraso-nic rolling electrochemical micromachining. *Chin. J. Aeronaut.* **2022**, *35*, 494–508.
12. Li, Y.; Geng, J.; Wang, Z.; Song, C.; Zhang, C.; Chen, D.; Wang, H. Influence of surface integrity on the fatigue performance of TiB2/Al composite treated byultrasonic deep rolling: Experime-nts and sim-ulations. *Compos. Part B Eng.* **2024**, *271*, 111160. [CrossRef]
13. Yuan, Z.; Qin, Y.; Deng, C.; Zheng, P. Synergistic effects of surface strengthening and surface micro-texture on aviation spherical plain bearing tribological properties. *Proc. Inst. Mech. Eng. Part J J. Eng. Tribol.* **2018**, *232*, 797–808. [CrossRef]
14. Yuan, Z.; Qin, Y.; Cheng, K.; Zhao, W.; Zheng, P. Investigation on surface morphology and tribological property generated by vibration assisted strengthening on aviation spherical plain bearings. *Proc. Inst. Mech. Eng. Part C J. Mech. Eng. Sci.* **2019**, *233*, 4091–4101. [CrossRef]
15. Bae, K.C.; Kim, D.; Kim, Y.H.; Oak, J.J.; Lee, H.; Lee, W.; Park, Y.H. Effect of heat treatment, building direction, and sliding velocity on wear behavior of selectively laser-melted maraging 18Ni-300 steel against bearing steel. *Wear* **2021**, *482*, 203962.
16. Meng, Y.; Deng, J.; Zhang, Y.; Wang, S.; Li, X.; Yue, H.; Ge, D. Tribological properties of textured surfaces fabricated on AISI 1045 steels by ultrasonic surface rolling under dry reciprocating sliding. *Wear* **2020**, *460*, 203488. [CrossRef]
17. Liu, Y.; Cui, H.; Liu, Y.; Zhao, X. Comprehensive Analysis of the Effect of Ultrasonic Surface Rolling Process on the Friction and Wear Properties of TB8 Titanium Alloy. *J. Mater. Eng. Perform.* **2023**, *32*, 9448–9459. [CrossRef]
18. Ye, H.; Chen, A.; Liu, S.; Zhang, C.; Gao, Y.; Li, Q.; Lv, J.; Chen, J.; Guo, H. Effect of ultrasonic surface rolling process on the surface properties of QAl10-3-1.5 aluminum bronze alloy. *Surf. Coat. Technol.* **2022**, *433*, 128126. [CrossRef]

19. Duan, Y.; Qu, S.; Jia, S.; Li, X. Effects of ultrasonic surface rolling processing on microstructure and wear properties of high-carbon high-chromium steel. *Surf. Coat. Technol.* **2021**, *422*, 127531. [CrossRef]
20. Meigui, Y.; Haiyan, Y.; Jiangqi, L. Effect of ultrasonic surface rolling process on the impact wear behavior of Inconel 690 alloy at 25 °C and 300 °C. *Surf. Topogr. Metrol. Prop.* **2022**, *10*, 025022.
21. Yin, M.; Zhang, L.; Huang, L.; Zhang, X. Effect of ultrasonic surface rolling process on the fretting tribocorrosion behaviors of Inconel 690 alloy. *Tribol. Int.* **2023**, *184*, 108451. [CrossRef]
22. Peng, Z.; Zhang, X.; Zhang, Y.; Liu, L.; Xu, G.; Wang, G.; Zhao, M. Wear resistance enhancement of Inconel 718 via high-speed ultrasonic vibration cutting and associated surface integrity evaluation under high-pressure coolant supply. *Wear* **2023**, *530*, 205027. [CrossRef]
23. Djalab, A.; Sari, M.R.; Haiahem, A.; Flamand, L. Mathematical modeling and statistical analysis of wear and surface roughness in contaminated dry rolling contacts. *J. Balk. Tribol. Assoc.* **2016**, *22 Pt 3*, 4593–4617.
24. Hansen, N. Hall–Petch relation and boundary strengthening. *Scr. Mater.* **2004**, *51*, 801–806. [CrossRef]
25. Dang, J.; Zhang, H.; An, Q.; Lian, G.; Li, Y.; Wang, H.; Chen, M. Surface integrity and wear behavior of 300M steel subjected to ultrasonic surface rolling process. *Surf. Coat. Technol.* **2021**, *421*, 127380. [CrossRef]
26. Li, G.; Qu, S.; Guan, S.; Wang, F. Study on the tensile and fatigue properties of the heat-treated HIP Ti-6Al-4V alloy after ultrasonic surface rolling treatment. *Surf. Coat. Technol.* **2019**, *379*, 124971. [CrossRef]

Disclaimer/Publisher's Note: The statements, opinions and data contained in all publications are solely those of the individual author(s) and contributor(s) and not of MDPI and/or the editor(s). MDPI and/or the editor(s) disclaim responsibility for any injury to people or property resulting from any ideas, methods, instructions or products referred to in the content.